

Isotope effects in the Hubbard-Holstein model within dynamical mean-field theory

P. Paci,¹ M. Capone,^{2,3} E. Cappelluti,^{2,3} S. Ciuchi,^{4,2} and C. Grimaldi^{5,6}

¹*International School for Advanced Studies (SISSA), via Beirut 2-4, 34014 Trieste, Italy*

²*SMC-INFM and Istituto dei Sistemi Complessi, CNR, via dei Taurini 19, 00185 Roma, Italy*

³*Dipart. di Fisica, Università "La Sapienza", P.le A. Moro 2, 00185 Roma, Italy*

⁴*Dipart. di Fisica, Università de L'Aquila, and INFM UdR AQ, 67010 Coppito-L'Aquila, Italy*

⁵*Ecole Polytechnique Fédérale de Lausanne, LPM, Station 17, CH-1015 Lausanne, Switzerland and*

⁶*DPMC, Université de Genève, 24 quai Ernest Ansermet, CH-1211 Genève 4, Switzerland*

(Dated: October 10, 2018)

We study the isotope effects arising from the coupling of correlated electrons with dispersionless phonons by considering the Hubbard-Holstein model at half-filling within the dynamical mean-field theory. In particular we calculate the isotope effects on the quasi-particle spectral weight Z , the renormalized phonon frequency, and the static charge and spin susceptibilities. In the weakly correlated regime $U/t \lesssim 1.5$, where U is the Hubbard repulsion and t is the bare electron half-bandwidth, the physical properties are qualitatively similar to those characterizing the Holstein model in the absence of Coulomb repulsion, where the bipolaronic binding takes place at large electron-phonon coupling, and it reflects in divergent isotope responses. On the contrary in the strongly correlated regime $U/t \gtrsim 1.5$, where the bipolaronic metal-insulator transition becomes of first order, the isotope effects are bounded, suggesting that the first order transition is likely driven by an electronic mechanism, rather than by a lattice instability. These results point out how the isotope responses are extremely sensitive to phase boundaries and they may be used to characterize the competition between the electron-phonon coupling and the Hubbard repulsion.

PACS numbers: 71.38.-k,63.20.Kr,71.38.Cn,71.38.Ht

I. INTRODUCTION

One of the most direct methods to establish the coupling of an electronic property with the dynamics of the underlying lattice is the isotope effect (IE), $\alpha_A = -d \ln A / d \ln M$, which probes the dependence of the electronic quantity A on the ion mass M . For example, the observation of a large IE on the superconducting transition temperature T_c has been an important evidence for a phonon-mediated pairing mechanism in conventional low-temperature superconductors. In the weak-coupling BCS model, the superconducting critical temperature is proportional to the Debye phonon frequency which scales as $M^{-1/2}$. The resulting IE on T_c , $\alpha_{T_c} = 1/2$, has been considered as one of the most important confirmation of the BCS theory.

The vanishingly small values of α_{T_c} in optimally doped high- T_c copper oxides superconductors has initially induced a large part of the scientific community to believe that the pairing mechanism in these compounds was mainly of electronic origin, and oriented the theoretical research towards purely electronic models, relegating the lattice to a secondary role. Later experimental investigations showed however that small values of α_{T_c} are peculiar of the optimal doping, whereas sizable values of α_{T_c} , even larger than the BCS prediction, were reported in the underdoped phase.¹ Furthermore, the improvement of the experimental accuracy has allowed recently to establish the presence of isotopic shifts also in several physical quantities different from the superconducting T_c .

Sizable isotope effects (IEs) have been indeed found on the zero temperature penetration depth $\lambda_L(0)$,^{2,3} on the Knight shift,⁴ on the nuclear quadrupole resonance,⁵

on the pseudogap temperature,⁶ and on the angular resolved photoemission spectra.⁷ These findings are particularly remarkable since the Migdal-Eliashberg theory of the electron-phonon interaction predicts vanishingly small IEs other than α_{T_c} . For example, according to the BCS description of the superconducting state, the zero temperature penetration depth is given by $\lambda_L(0) = (m^*/n_s)^{1/2}$, where n_s is the density of the condensate and m^* is the effective electron mass. According to the Migdal-Eliashberg theory, $m^* = (1 + \lambda)m$, where m is the bare band mass and λ is the electron-phonon coupling constant. Since λ is independent of the ion mass, the isotope effect on the penetration depth is expected to be zero, in contrast with Refs. 2,3.

The completely anomalous set of isotope dependences signals a relevant electron-phonon coupling, but at the same time highlights that the interplay with strong correlations and possibly with other features of the cuprates needs to be taken into account. Different theoretical models have been proposed to account for these anomalous IEs.^{8,9,10,11,12,13,14} The analysis has been mainly concentrated on purely electron-phonon narrow-band systems, as the Holstein model which however neglects possible effect of the anisotropy of the electron-phonon interaction considered in Ref. 15.

The IEs on m^* in interacting electron-phonon systems in the absence of electron-electron interactions have been investigated in details in Refs. 8,9,10. More recently, the ability of the IEs in revealing different physical regimes of electron-phonon systems has been discussed in Ref. 16 where remarkable anomalous IEs on m^* and on the dressed phonon frequency Ω_0 were reported as the system enters in a polaronic regime. In order to focus on

the metallic properties and to clarify the origin of these anomalous IEs, however, a spinless Holstein model in the DMFT approximation was considered there, which enforces the metallic character in the whole space of parameters.

In the opposite case of strong correlations the electron-phonon interaction in the weak-intermediate limit has been treated for instance by means of an adiabatic theory on small clusters,¹⁷ or of coherent potential approximation.¹⁸ In this case the IE reflects in a smooth modification of high energy features such as the Hubbard bands. In the strongly correlated antiferromagnetic phase IEs on the single hole spectral properties have been also analyzed with diagrammatic quantum Monte Carlo techniques.¹⁹

The scope of this paper is to provide a nonperturbative analysis of the isotope effects on different observables in a regime in which strong correlation and intermediate/strong electron-phonon interaction coexist. To this aim we employ the dynamical mean-field technique (DMFT), which is powerful tool to investigate the non-perturbative regimes of strongly correlated and electron-phonon systems. In particular, in this paper we consider the metallic regime of the Hubbard-Holstein model, deliberately excluding broken-symmetry phases. We also limit ourselves to the half-filled systems, where in DMFT the correlation-driven Mott transition or the electron-phonon driven pairing transition take place as one or the other coupling becomes large, and we follow the behavior of the isotope effects when these phase boundaries are approached. It is well known that DMFT becomes exact only in the limit of infinite coordination number, and it has to be viewed as an approximate method in finite dimensions. Yet, DMFT allows us to access the full local quantum dynamics, and to deal with many different energy scales. Moreover the assumption of a local self-energy, implicit in the DMFT, makes this technique not suitable to investigate the momentum dependence of the physical quantities. This is for instance the case of Frölich-like electron-phonon Hamiltonians and of the long-range Coulomb interaction, which gives rise to important screening effects here neglected.²⁰ This is also the case of the momentum dependence of the electron-phonon interaction induced by the electronic correlation itself^{21,22,23}, which cannot be properly take into account within the context of the DMFT.

A general belief is that the electronic correlation competes with the electron-phonon interaction leading to a reduction of the phonon effects on the electronic properties with a consequent decrease of the magnitude of the possible IEs. We show that in particular regimes, close to phase boundaries, the Hubbard repulsion can actually *enhance* the dependence of many physical quantities on the phonon frequency, yielding an increase of the IEs. Indeed the isotope effects turns out to be extremely sensitive to the closeness of metal-insulator transitions, and emerge as a tool to investigate the physics underlying the different regimes of the phase diagram.

This paper is organized as follows. In Sec. II we introduce the Hubbard-Holstein model and the dynamical mean field method. In Sec. III and Sec. IV we report our results for the weakly correlated and strongly correlated regimes, respectively, while a study of the IEs as a function of the Hubbard- U repulsion is the subject of Sec. V. The conclusions are summarized in Sec. VI

II. OUR APPROACH

The Hubbard-Holstein model is defined by the Hamiltonian:

$$H = -t \sum_{\langle ij \rangle \sigma} c_{i\sigma}^\dagger c_{j\sigma} + U \sum_i n_{i\uparrow} n_{i\downarrow} + g \sum_{i\sigma} n_{i\sigma} (a_i + a_i^\dagger) + \omega_0 \sum_i a_i^\dagger a_i, \quad (1)$$

where t is the hopping amplitude between nearest neighboring sites, U is the Hubbard electron-electron repulsion, g is the electron-phonon matrix element, and ω_0 the Einstein phonon frequency.

We can identify three independent dimensionless parameters, the electron-phonon coupling constant $\lambda = 2g^2/(\omega_0 t)$, the adiabatic ratio $\gamma = \omega_0/t$, which parametrizes the role of the lattice quantum fluctuations, and the dimensionless Hubbard repulsion U/t . It is important to note that $\omega_0 \propto 1/\sqrt{M}$ and $g \propto 1/\sqrt{M\omega_0}$, where M is the ionic mass, so that the only physical quantity which depends on M is the adiabatic ratio γ . Finite IEs stem thus from an explicit dependence on γ and they are hence a direct signal of the role of the lattice quantum fluctuations. The locality of the interaction terms makes the Hubbard-Holstein model particularly suitable to be investigated by dynamical mean-field theory.²⁴ In this approach the spatial fluctuations are frozen, i.e., all the lattice sites are assumed to be equivalent, but the local electron and phonon dynamics are fully accounted for. In this sense the method generalizes to a quantum framework the classical mean-field theories, and it becomes exact in the infinite coordination limit. Hence the lattice model is mapped onto a quantum impurity model in which an interacting site is embedded into a non-interacting bath, whose spectral function has to be self-consistently determined. In our case, the impurity site displays both Coulomb repulsion and a coupling to a local phonon. The self-consistency equation contains all the information about the original lattice model through the bare density of states. As often, here we consider an infinite coordination Bethe lattice with half-bandwidth t ,²⁵ which reproduces the finite bandwidth of finite-dimensional systems. For the normal paramagnetic phase, the self-consistency condition on the Bethe lattice reads

$$\Delta(\omega) = \frac{t^2}{4} G(\omega), \quad (2)$$

where G is the Green's function on the impurity site, which corresponds to the local component of the lattice Green's function, and Δ is the bath hybridization function. Within DMFT the electron and phonon self-energies are local, i.e., momentum independent.

To solve the impurity model we use the exact diagonalization method,²⁶ in which the dynamical DMFT bath is described in terms of a finite set N_s of Anderson impurity levels, while a finite cut-off is imposed on the total number N_{ph} of the phononic Hilbert space. Typical values we considered are $N_s = 9, 10$, and $N_{\text{ph}} \sim 20$. Both these quantities were varied to check the effective stability of the results. The self-consistent DMFT set of equations was solved in the Matsubara space where a fictitious temperature \tilde{T} plays the role of an energy cut-off. Particularly small value of \tilde{T} up to $\tilde{T}/t \sim 1/400$ were needed to ensure a high accuracy of our results.

In this paper we investigate unconventional IEs on both single-particle and two-particle quantities. In particular, concerning the one-particle properties, we focus on the quasi-particle spectral weight Z , which in DMFT coincides with the inverse of the effective electronic mass m^*/m due to the momentum independence of the self-energy Σ

$$Z = \left(1 - \frac{\partial \Sigma(\omega_n)}{\partial \omega_n} \Big|_{\omega_n=0} \right)^{-1}, \quad (3)$$

and on the renormalized phonon frequency Ω_0 obtained as²⁷

$$\left(\frac{\Omega_0}{\omega_0} \right)^2 = - \frac{2D^{-1}(\omega_m = 0)}{\omega_0}. \quad (4)$$

In the above expressions, $\Sigma(\omega_n)$ is the electronic self-energy and $D(\omega_m)$ is the phonon propagator $D(\omega_m) = -\langle x(\omega_m)x(-\omega_m) \rangle$, where $x = (a + a^\dagger)$ is the dimensionless lattice coordinate operator. ω_n and ω_m are respectively fermionic $\omega_n = \pi\tilde{T}(2n + 1)$ and bosonic $\omega_m = 2\pi\tilde{T}m$ Matsubara frequencies. In practice Z is computed by linearly extrapolating from the first Matsubara frequency.

The knowledge of the renormalized phonon frequency Ω_0 allows us to evaluate also the static component of the local charge susceptibility $\rho = \rho(\omega_m = 0)$, where $\rho(\omega_m) = \langle n(\omega_m)n(-\omega_m) \rangle$, n being the density operator on the impurity. It is indeed easy to prove that $\rho = (1 - \omega_0^2/\Omega_0^2)/\lambda t$. We evaluate also the local static spin susceptibility $\chi = \chi(\omega_m = 0)$ for the spin response function $\chi(\omega_m) = \langle S_z(\omega_m)S_z(-\omega_m) \rangle$, where $S_z = (1/2)\sum_{\alpha\beta} c_\alpha^\dagger \sigma_{\alpha\beta}^z c_\beta$ is the z -component of the local electron spin ($\hat{\sigma}^z$ being the Pauli matrix $\hat{\tau}_3$). Finally, we consider also the local lattice probability distribution function $P(x) = |\langle \phi_0|x \rangle|^2$, where $|x\rangle$ is the eigenstate of the lattice coordinate operator x . In our exact diagonalization approach we can evaluate $P(x) = \sum_{n,m} \psi_n(x)\psi_m(x)\langle \phi_0|n\rangle\langle m|\phi_0\rangle$, where $|\phi_0\rangle$ is the ground state, $|n\rangle$ are the eigenstates of the harmonic oscillator and $\psi_n(x)$ the corresponding eigenfunctions.

Despite its simplicity, the Hubbard-Holstein model has quite a rich phase diagram, in which different phases and regimes appear. In order to have a better comparison between the different regimes, we organize our discussion according to degree of correlation. In the next section we focus on the weakly correlated regime of the Holstein-Hubbard model, where the presence of the on-site Hubbard repulsion changes only quantitatively the results of the pure Holstein spinful model, but it does not give rise to new features. We then discuss in section IV the regime of strong electronic correlation where the interplay between electron-phonon and electron-electron interaction induces qualitative changes on the behavior of the IEs.

III. WEAKLY CORRELATED REGIME

Already in the absence of correlation, the introduction of the spin degeneracy introduces additional physics with respect to the spinless system, whose isotope effects have been studied in Ref. 16. In the spinless case indeed the polaron crossover is not associated with a metal-insulator transition (MIT) which is only asymptotically approached for $\lambda \rightarrow \infty$. The persistence of a metallic character in the polaronic phase is reflected in the finite value of both the quasi-particle weight and the renormalized phonon frequency.²⁷ On the other hand in the spinful case the residual attractive interaction between the electronic or polaronic charges leads to the possibility to form a insulating phase of localized pairs which in the adiabatic regime ($\gamma \ll 1$) are accompanied by strong lattice deformation (bipolarons).²⁸ This occurs within the DMFT approximation for λ larger than a finite critical value where the quasi-particle weight vanishes at λ_{MIT} signaling a pair-MIT.²⁹ In the adiabatic limit ($\gamma = 0$) the pair-MIT has a precursor in the phonon softening which occurs at λ_{ph} .³⁰ As the bare phonon frequency is increased, the phonon softening tends to occur more closely to the pair-MIT.³¹

In Fig. 1 we show the quasi-particle spectral weight Z , the renormalized phonon frequency Ω_0 , the local static spin susceptibility χ and the local static charge susceptibility ρ as functions of the electron-phonon coupling λ for different weak-intermediate values of the Hubbard repulsion U and for adiabatic ratios $\gamma = 0.1, 1.0$. χ_0 and ρ_0 represent respectively the local spin and charge susceptibility in the absence of electron-phonon and Hubbard interaction. As mentioned above, the main difference here with respect to the spinless Holstein model is the possibility to form local bipolaronic pairs of electrons with opposite spin. This leads to a metal-insulator transition at a finite electron-phonon coupling λ_{MIT} where $Z \rightarrow 0$. The metal-insulator transition is accompanied by a softening of the phonon frequency $\Omega_0 \rightarrow 0$ for a value λ_{ph} of the electron-phonon very close to λ_{MIT} , followed by a sudden increase for $\lambda > \lambda_{\text{ph}}$.^{27,31,32}

The approach to the bipolaronic metal-insulator transition is reflected also in the two-particle quantities χ

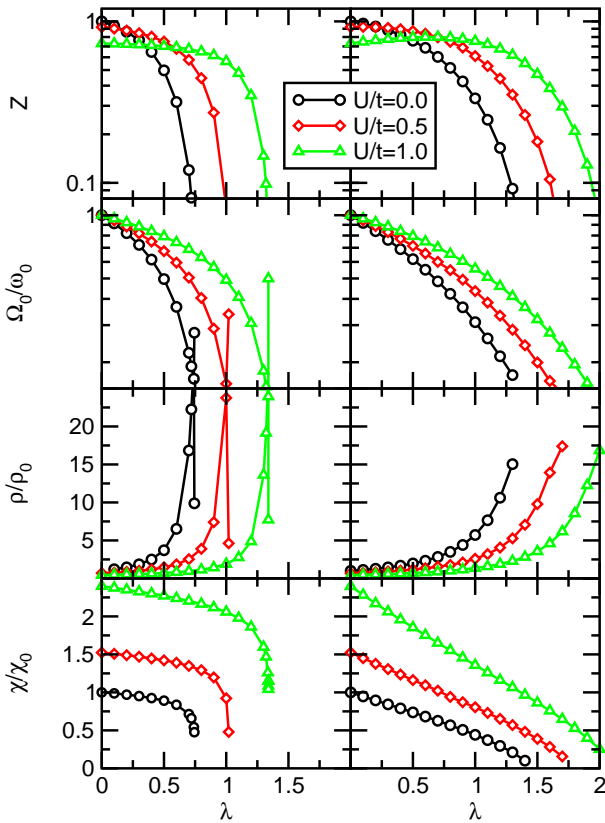


FIG. 1: (color online) Behavior of the quasi-particle spectral weight Z , the renormalized phonon frequency Ω_0 , the local static charge susceptibility ρ and the local static spin susceptibility χ as functions of the electron-phonon coupling λ for different weak-intermediate values of the Hubbard repulsion U . In the left panel the curves are plotted for the adiabatic ratio $\gamma = 0.1$ while in the right panel the adiabatic ratio is $\gamma = 1.0$.

and ρ . In particular, the increase in the number of singlet local electron pairs close to the transition leads to a suppression of the local spin susceptibility and to an enhancement of the local charge susceptibility, so that χ has a sharp drop whereas ρ nearly diverges at λ_{ph} .

In this context the Hubbard repulsion gives rise to a further reduction of metallic properties at small λ (decrease of Z) while, on the other hand, it disfavors double occupancy leading to a shift to larger λ of the critical values of the el-ph coupling and to an increase (decrease) of the spin (charge) susceptibility. Finally, increasing the quantum lattice fluctuations ($\gamma = 1.0$, right panels) leads to a further increase of the critical electron-phonon couplings.

In Fig. 2 we show the corresponding isotope coefficients

$$\alpha_X = -\Delta \log X / \Delta \log M = (1/2)\Delta \log X / \Delta \log \gamma, \quad (5)$$

where X is Z , Ω_0 , χ and ρ . We have chosen to compute the IEs using a finite value $\Delta\gamma/\gamma = 0.15$.

The behavior of IEs approaching λ_{MIT} and λ_{ph} is

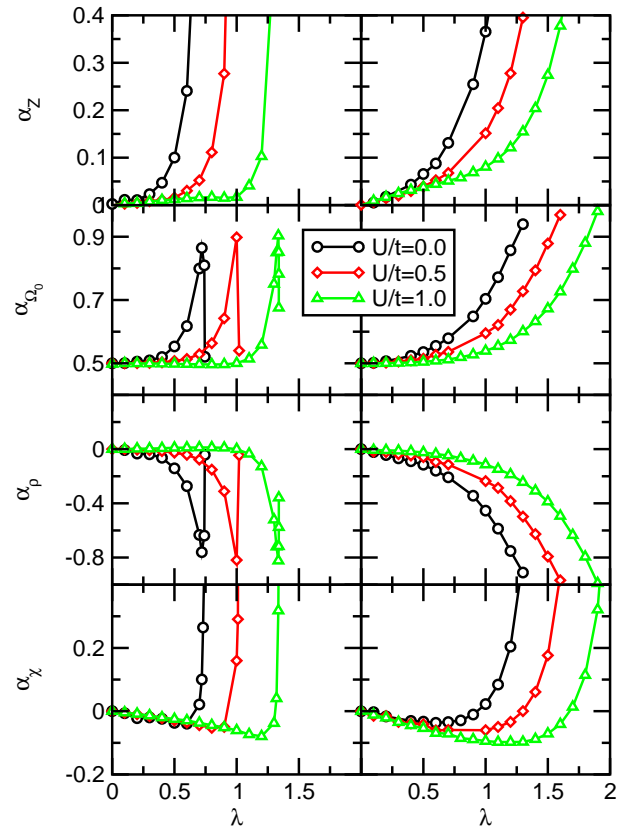


FIG. 2: (color online) Plot of the isotope coefficients for the same quantities defined in Fig. 1.

depicted in Fig. 2. The most striking effect is the near *divergence* of the isotope coefficients as the system approaches the pairing metal-insulator transition. As a matter of fact, while α_Z has a true divergence as $\lambda \rightarrow \lambda_{MIT}$, for the isotope effects on the other quantities the divergence is cut-off by the not complete suppression of charge fluctuations. From the practical point of view however both the MIT and bipolaronic instabilities are accompanied by a huge increase of the magnitude of the anomalous isotope effects.

The key point to understand this issue is that an isotopic shift of ω_0 is reflected in a finite shift to higher λ of both the bipolaronic MIT (λ_{MIT}) and the phonon softening (λ_{ph}). It obviously descends from Eq. (5) that the divergence of a quantity is accompanied by a divergence to $-\infty$ of the corresponding isotope coefficient α , while a positively divergent isotope coefficient is associated to a vanishing observable. According this view we can understand the behaviors of Fig. 2. Namely we find that $\alpha_Z \rightarrow \infty$ as $Z \rightarrow 0$ at λ_{MIT} and α_χ nearly diverges as χ rapidly drops at λ_{MIT} . In similar way the near vanishing of Ω_0 and the near divergence of ρ , at λ_{ph} are reflected in $\alpha_{\Omega_0} \rightarrow +\infty$ and $\alpha_\rho \rightarrow -\infty$. The following drop of α_{Ω_0} and the jump of α_ρ for $\lambda > \lambda_{ph}$ reflect the sharp behavior shown in Fig.1 of the corresponding quantities.

Increasing U leads to an increase of λ_{MIT} , while in-

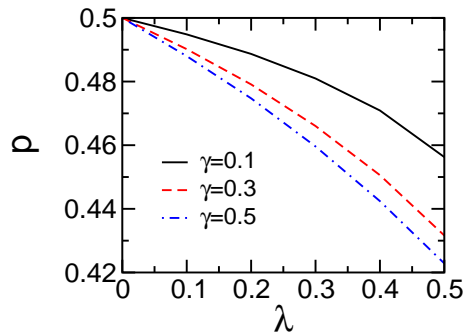


FIG. 3: (color online) Behavior of single occupation number $\rho = |\langle \uparrow | \phi_0 \rangle|^2 + |\langle \downarrow | \phi_0 \rangle|^2$ as function of λ in the weak el-ph coupling regime ($\lambda \simeq 0.5$) for different adiabatic ratio γ and for $U = 0$.

creasing ω_0 determines an overall smoothing of these features. An interesting point to be noted here is the non monotonic behavior of the IE on the spin susceptibility χ , which shows a negative sign at small λ before approaching a near divergence towards $+\infty$ close to the metal-insulator transition. On the contrary α_ρ remains negative up to λ_{ph} . The negative sign of α_χ and α_ρ for small λ can be understood in a perturbative framework. The electron-phonon interaction introduces a positive Stoner-like contribution to the effective spin susceptibility:

$$\chi = \frac{\chi_0}{1 - I_{\text{el-el}} + I_{\text{el-ph}}^{\chi}}, \quad (6)$$

where $I_{\text{el-el}} \propto U$ arises from the electron-electron repulsion and the electron-phonon term $I_{\text{el-ph}}^{\chi} \propto \gamma\lambda$ takes into account the explicitly isotope dependence due to the finite bandwidth and vertex corrections arising from the electron-phonon interaction.^{9,33} In the same RPA fashion the charge susceptibility reads

$$\rho = \frac{\rho_0}{1 + I_{\text{el-el}} + I_{\text{el-ph}}^{\rho}}, \quad (7)$$

where $I_{\text{el-ph}}^{\rho} = -\lambda + I_{\text{el-ph}}^{\chi}$. Thus at a perturbative level the only source of IE in ρ and χ comes from $I_{\text{el-ph}}^{\chi}$, which can be shown to be the same as in both quantities leading to the *same* negative IE.

The sign of the isotope coefficient on the spin susceptibility reflects thus two different physical regimes where lattice fluctuations triggered by ω_0 play a different role. Namely, in the perturbative small λ regime lattice fluctuations disfavor single spin occupancy (Fig. 3), leading to a decrease of χ and to a negative isotope coefficient. On the other hand the physics in the $\lambda \lesssim \lambda_{\text{MIT}}$ region is dominated by the proximity to the bipolaronic MIT. In this context lattice fluctuations relax the phonon-induced electron trapping favoring the unpaired spin singlet states. Along this line the sign of the isotope coefficient on χ can be thus used as a useful trademark to characterized the different physical regimes. The ability of the IE to characterize the physical properties of differ-

ent regimes will be even more remarkable in the strongly correlated regime.

IV. STRONGLY CORRELATED REGIME

In the previous section we have seen that for small U the physical properties of the system are qualitatively similar to those of the pure Holstein model, where turning on a small Coulomb repulsion leads essentially only to an increase of the critical value of λ for bipolaron pairing. The situation is significantly changed in the strongly correlated regime in which the Hubbard repulsion exceeds the electron-phonon coupling. In this case a more reasonable starting point is the physics of the pure Hubbard model whose metallic region, close to the Mott transition, can be described in terms of a narrow resonance at Fermi level accompanied by the two high-energy Hubbard subbands. In this framework the electron-phonon interaction has two opposite effects: on one hand it provides a further source of scattering which would decrease the quasi-particle scattering weight Z ; on the other hand it acts as a effective attraction between the electrons, competing with the Hubbard repulsion.³⁴ In the strongly correlated regime, when the reduction of the effective repulsion prevails over the electron-phonon renormalization of the quasi-particle properties, increasing λ leads to an enhancement of Z .^{31,34}

Another interesting feature of the Hubbard-Holstein model pointed out in Ref. 31 in the strongly correlated regime is the change of the order of the bipolaronic MIT at $\gamma = 0.1$. The bipolaronic transition, which is continuous (second order) for $U/t \lesssim 1.5$, becomes indeed discontinuous (first order) for $U \gtrsim 1.5$. In this latter regime all the observable have thus a jump at λ_{MIT} . The evolution from a second order to a first order transition has been discussed in terms of a Landau-Ginzburg theory where the first/second order transition is driven by the local lattice configuration.³⁵ From a numerical point of view, however, it is hard to distinguish, on the basis of observables like Z or Ω_0 a first order transition from a sharp second order one. We show that the analysis of the phonon IE is a powerful tool to distinguish in a very clear way the first order or the second order character of the bipolaronic MIT. This is even more interesting since, as we are going to show, the first order transition is not related to a phonon mechanism while it is probably of a electronic origin.

In Fig. 4 we show Z , Ω_0 , χ and ρ as function of λ in the regime of strong correlation for $\gamma = 0.1$ and for $\gamma = 1.0$. As mentioned above, in this strongly correlated regime, increasing λ , as long as the system does not reach a bipolaronic regime, results in a reduction of the effective Hubbard repulsion and in an increase of Z . It is however interesting to note that the behavior of the other quantities, namely Ω_0 , χ and ρ , as function of λ and U does not change qualitatively with respect to the weakly correlated case. Concerning the character of the

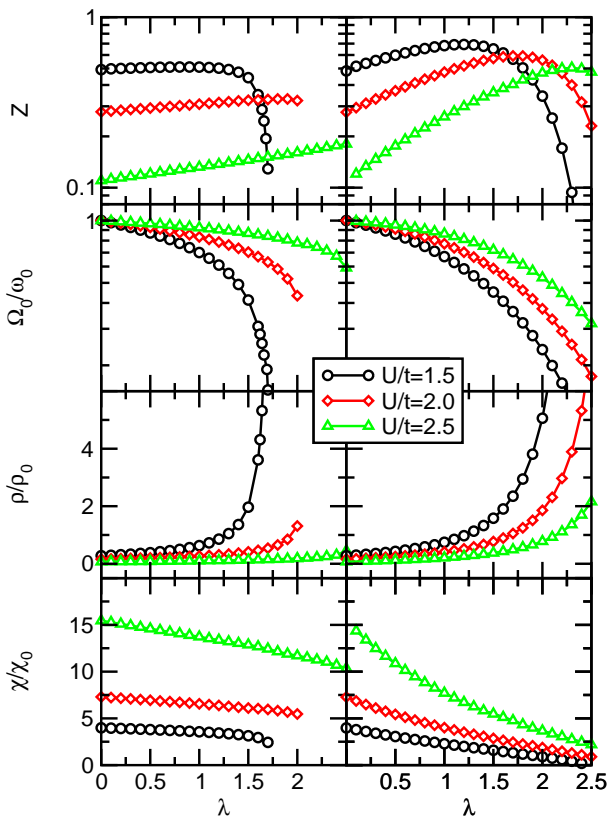


FIG. 4: (color online) Behavior of the quasi-particle spectral weight Z , of the renormalized phonon frequency Ω_0 and of the charge and spin susceptibilities, ρ and χ , as functions of the electron-phonon coupling λ for different intermediate-strong values of the Hubbard repulsion U . In the left panel the curves are plotted for the adiabatic ratio $\gamma = 0.1$ while in the right panel the adiabatic ratio is $\gamma = 1.0$.

bipolaronic MIT, we find that the transition is always of the second order for any U at $\gamma = 1.0$. On the other hand, due to the lack of precursor effects in the metallic phase, it is hard to predict the character of the transition at $\gamma = 0.1$.

The corresponding IEs on the quantities Z , Ω_0 , χ and ρ is reported in Fig. 5. We note a qualitatively different behavior of the isotope coefficients in the strongly correlated regime at $\gamma = 0.1$ as compared with the weak U regime and (partially) with the case $\gamma = 1.0$. Let us discuss for the moment the highly correlated cases $U/t = 2.0, 2.5$. Most striking is the behavior of the phonon and of the charge susceptibility isotope coefficient which shows a trend diametrically opposite to the weak- U case, namely a marked *reduction* (increase) of α_{Ω_0} (α_ρ) to be compared with the divergences $\alpha_{\Omega_0} \rightarrow \infty$, $\alpha_\rho \rightarrow -\infty$ for small U . Among the other anomalous features we note a typical downturn of α_Z as function of λ , which is less marked as U increases. On the contrary, the upturn of the isotope coefficient on the spin susceptibility which is evident at small U is here absent. Quite interesting is also the $U/t = 1.5$ case which is very close

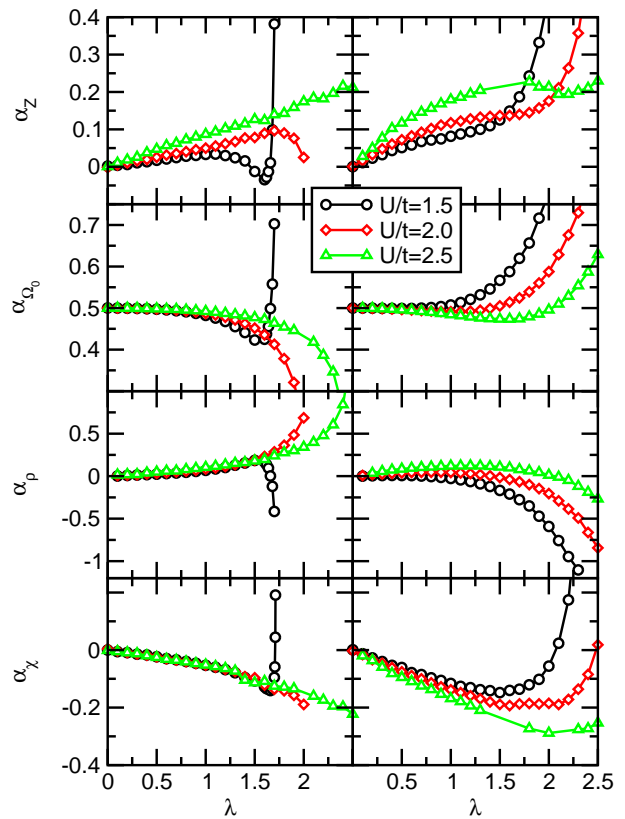


FIG. 5: (color online) Plot of the isotope coefficients for the same quantities reported in Fig. 4.

to the value where the bipolaron MIT changes from the second order to the first order. In this case the IEs show similar trends ($\alpha_{\Omega_0} < 0.5$, $\alpha_\rho > 0$, downturn of α_Z) as for the first order cases in a large range of λ , with a final upturn (downturn for α_ρ) towards the characteristic divergences of the second order. This trend is clearly visible also at $\gamma = 1.0$ (although the bipolaronic transition is always of the second order) pointing out an underlying tendency towards a first order instability. The larger amount of the lattice fluctuations in this case as compared with $\gamma = 0.1$ prevents however the occurrence of the first order instability and enforces the second order character.

As we are going to show, the physical origin of these anomalous behaviors can be related to different phonon regimes, although they do not rule directly the change between the first and second order character of the transition. In order to clarify in more details this issue we evaluate the local lattice probability distribution function (PDF) $P(x)$ which provides information about the lattice wavefunction of the ground state. In Fig. 6 (upper panel) we show the PDF for two representative cases characterized by significant lattice distortions induced by the electron-phonon interaction, resulting in a non-gaussian $P(x)$. In the strictly adiabatic case, polaronic effects for instance are reflected by a bimodal shape of $P(x)$, where the two maxima are associated to different electron oc-

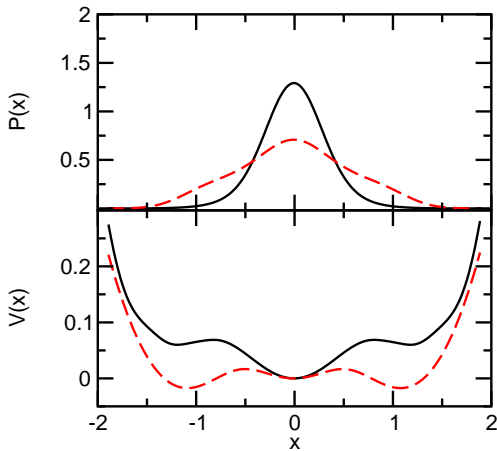


FIG. 6: (color online) PDF lattice function $P(x)$ and lattice potential $V(x)$. Solid black line: $U/t = 2.0$, $\lambda = 2.0$, dashed red line: $U/t = 1.5$, $\lambda = 1.7$.

cupancies (e.g., in spinless systems $n = 0$ and $n = 1$, in spinful systems $n = 0$ and $n = 2$). The broadness of these structures induced by quantum lattice fluctuations however can make hard to resolve the effective extent of the polaronic lattice distortions. To overcome this problem we extract an “effective” lattice potential $V(x)$ by solving the inverse Schrödinger problem

$$\left[-\frac{1}{2M} \nabla^2 + V(x) \right] \bar{\psi}(x) = \omega_0 \bar{\psi}(x), \quad (8)$$

where $\bar{\psi}(x) = \sqrt{P(x)}$ and M is the atomic mass. Fig. 6 shows the lattice distribution function $P(x)$ and the corresponding lattice potential $V(x)$ for two representative cases where the multi-valley structure of $V(x)$ is not reflected in the shape of $P(x)$. We stress that the above defined $V(x)$ reproduces the physical lattice potential only in the strict adiabatic limit $\gamma \rightarrow 0$. It can be considered however to be still a valid approximation at finite and small γ providing thus useful insights for the true (unknown) lattice potential.

In Fig. 7 we report the evolution of the lattice potential $V(x)$ as function of λ for three representative cases of the Hubbard repulsion, $U/t = 1.0, 1.5, 2.0$, and for $\gamma = 0.1$. All the shown λ 's belong to the metallic phase. The largest value of λ , in each panel of the left side of Fig. 7, corresponds to the MIT.

The first case (panel a) shows, in agreement with a second-order transition scenario, a continuous flattening of the lattice potential as λ increases. This picture shows in the clearest way the lattice instability at $\lambda_{\text{ph}} \simeq 1.3$, where the quadratic term of $V(x) \simeq a_2 x^2 + a_4 x^4 + \dots$ vanishes and the renormalized phonon frequency $\Omega_0 \rightarrow 0$. For $\lambda_{\text{ph}} < \lambda < \lambda_{\text{MIT}}$ the system is still metallic and a double-well structure of the lattice potential is developing. This corresponds to the phonon hardening back shown in Fig. 1. The electronic metal-insulator transition occurs for $\lambda_{\text{MIT}} > \lambda_{\text{ph}}$ when the double-well potential is already established and the MIT is caused by

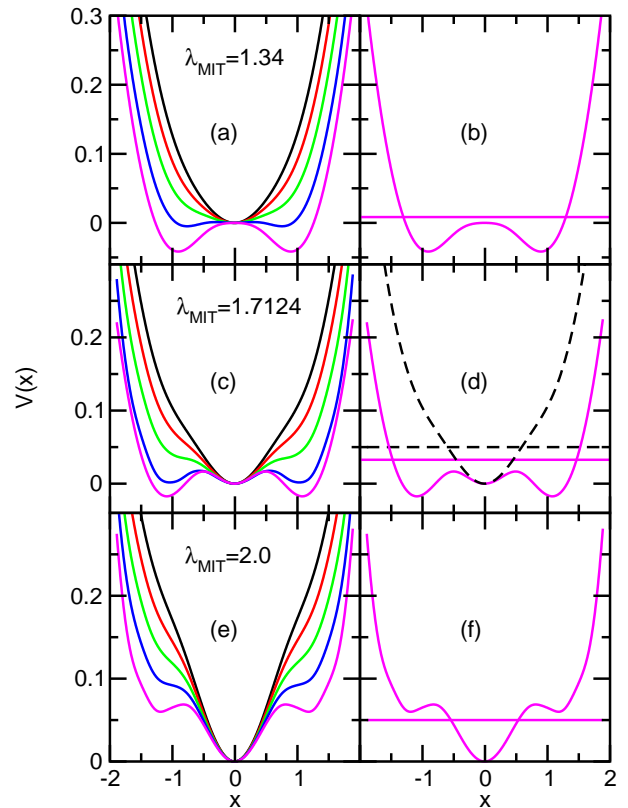


FIG. 7: (color online) Lattice potential $V(x)$ in different physical regimes. Upper panels: $U/t = 1.0$, $\lambda = 1.0, 1.1, 1.2, 1.3, 1.34$; (right: $\lambda = 1.34$). Middle panels: $U/t = 1.5$, $\lambda = 1.4, 1.5, 1.6, 1.7, 1.71246$; (right: $\lambda = 1.4, 1.71246$). Lower panels: $U/t = 2.0$, $\lambda = 1.6, 1.7, 1.8, 1.9, 2.0$; (right: $\lambda = 2.0$). The horizontal lines in panels b,d,f marks the zero point lattice energy for the corresponding lattice potential.

the vanishing of coherent tunneling between the two minima. A crucial role is played by the zero point phonon energy $\omega_0/2$ (horizontal lines in panel b) which favors tunneling processes. In particular, in the latter situation where the double-well is already formed, an increase of $\omega_0 \rightarrow \omega_0 + \Delta\omega_0$, due to an isotope shift, further enhances the metallic character, enhancing Z and resulting in a positive isotope coefficient on Z . At the same time the system, increasing ω_0 , will probe a less shallow potential (panel b) resulting in a stronger hardening of Ω_0 than the harmonic one and leading to $\alpha_{\Omega_0} > 0.5$.

A more complex situation is found for $U/t = 1.5$. Here, more than a softening of the quadratic term $a_2 x^2$, increasing λ the lattice potential $V(x)$ presents two flat regions at finite x which evolve first in two relative minima and then in two absolute minima lower than the central one (panel c). In this framework we distinguish two regimes. The first one is when the zero point energy is roughly lower than the flat regions (or minima) of the potential ($\lambda \lesssim 1.6$); in this situation increasing ω_0 makes the lattice wave-function more distorted, the metallic character is reduced and the phonon energy is

softened with respect to the harmonic one. This phenomenology is thus reflected in the downturn of α_Z and of $\alpha_{\Omega_0} < 0.5$. A second regime is reached for λ closer to the MIT ($\lambda \gtrsim 1.6$): here the minima are lower than the zero point energy, a phenomenology similar to the double-well potential is restored and $\alpha_Z > 0$, $\alpha_{\Omega_0} > 0.5$.

The results for $U/t = 2.0$ (panels e,f) are essentially similar to those for $U/t = 1.5$ for small λ . Here however the first-order metal-insulator transition occurs well before the relative minima at finite x reach the range of the zero point energy. As a consequence the previous considerations apply, namely α_Z shows an downturn (but it still remains finite) and $\alpha_{\Omega_0} < 0.5$.

The evolution of the lattice potential as function of U and λ sheds interesting light on the origin of the first-order/second-order character of the MIT. It has been indeed claimed that both the second-order at small U and the first-order transition at large U could be related to a phonon-driven mechanism.³⁵ In a phonon-driven Ginzburg-Landau theory the character of the transition is thus determined by the dependence of the free energy on the lattice coordinate, $F(x) \approx a_2 x^2/2 + a_4 x^4/4 + a_6 x^6/6$, which in the adiabatic limit reduces to the lattice potential $V(x)$. The second-order transition at small U is thus associated with the development of a double-well potential which occurs for $a_2 < 0$ and $a_4, a_6 > 0$, whereas a first order one is expected to correspond to a three-well structure with absolute minima at $x_0 \neq 0$, condition realized for $a_2, a_6 > 0$, $a_4 < -\sqrt{4a_2 a_6}$. Our results shown in Fig. 7 confute however this picture.

At $U \lesssim 1.5$ the second order MIT transition occurs *after* the development of the double well in $V(x)$. MIT here is indeed a by-product of the lattice distortions as was shown by adiabatic analysis of Ref. 30 and is due to the vanishing of the coherent tunneling processes between the minima of two double-well lattice potential.

For $U \gtrsim 1.5$ instead the developing of the three-well shape of the lattice potential is not sufficient to explain the first-order character since the MIT occurs *before* the local minima with finite lattice distortions at $x \neq 0$ become absolute minima. Moreover the energy of the local minima at the transition become higher and higher in energy as U increases, precisely where the first-order character becomes more marked. These considerations suggest thus that the origin of the first-order metal-insulator transition in the strongly correlated regime is likely ascribed to an electronic origin more than some phonon-driven instability. An intrinsic difference between the weakly and the strongly correlated metallic phase is the presence of a spin-singlet character in the metallic case pointed out by the presence of the Hubbard bands coexisting with the Kondo peak in the strongly correlated regime. If the metallic state has a pronounced spin-singlet character the transition to a bipolaronic pair state (which is instead a charge pseudo-spin singlet) can be viewed as a level crossing between this two different electronic states therefore leading to a first order transition.

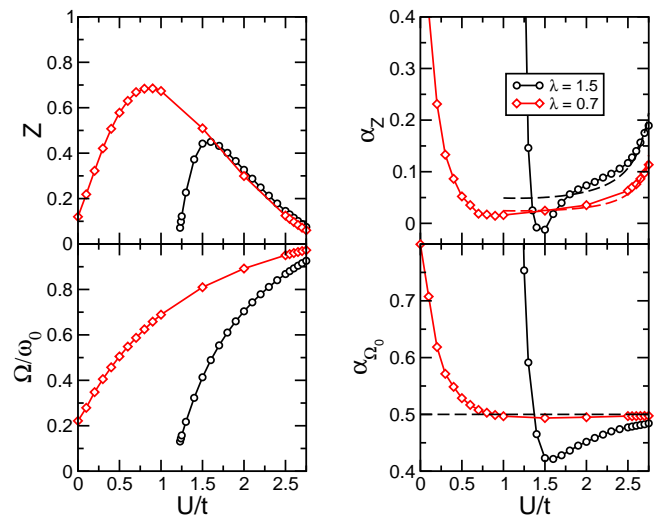


FIG. 8: (color online) Left panel: quasi-particle spectral weight Z and renormalized phonon frequency Ω_0 as functions of Hubbard repulsion U for two different $\lambda = 0.7$ (empty diamonds) and $\lambda = 1.5$ (empty circles). Right panel: the corresponding IEs α_Z and α_{Ω_0} . All curves are plotted for $\omega_0/t = 0.1$. In the right-top panel are also shown the analytical behavior predicted by Eq. (9) (dashed lines) by using, respectively, $U_c/t = 2.87$ for $\lambda = 0.7$ and $U_c/t = 2.90$ for $\lambda = 1.5$.

V. U-DEPENDENCE

In the previous section we have analyzed in details the behavior of the IEs on the physical quantities as function of the electron-phonon coupling λ . We have shown in particular that the IEs are quite sensitive to the different regimes of the electronic correlations, and we have distinguished the weak from the highly correlated regime. The aim of this section is to address this issue in more details by studying the dependence of the IEs on the Hubbard repulsion U . We shall focus on the IE on the quasi-particle spectral weight Z and on the renormalized phonon frequency Ω_0 which show the most characteristic features. We consider two values of λ , representative of two different physical regimes: $\lambda = 0.7$, for which the system is far from the bipolaronic phase even in the absence of any Hubbard repulsion; and $\lambda = 1.5$ for which value instead the ground state is a bipolaronic insulator at $U = 0$. In this case one needs a finite value of the Hubbard repulsion ($U \lesssim 1.25$) to contrast the el-ph driven attraction and to restore the metallic character. Both the cases of course undergo a Mott metal-insulator transition as U approaches some critical value U_c .

In Fig. 8 we report the evolution of the quasi-particle spectral weight Z and of the renormalized phonon frequency Ω_0 as functions of U for the two chosen λ . Let us discuss first the behavior of Ω_0 , which shows a monotonic behavior for $\lambda = 0.7$. This trend is representative for the generic case of weak electron-phonon coupling: due to the suppression of the double/empty sites, increasing U

leads to a reduction of the charge fluctuations and to the consequent enhancement of the renormalized phonon frequency Ω_0 which results less screened. More intriguing is the analysis of Z which, unlike the pure Hubbard model, shows a non-monotonic behavior as function of U . In the previous section we have discussed how, in the strongly correlated regime close to the Mott MIT, switching on the electron-phonon interaction leads to an increase of Z . This trend has been explained as a result of the competition between the attractive el-ph coupling and the repulsive Hubbard term.^{31,34} Fig. 8 shows that a similar mechanism applies also close to the bipolaron MIT where the phonon-driven attraction is the strongest interaction, and the Hubbard repulsion partially counteracts it, so that Z increases with the repulsion for small U . For larger U however the repulsion overcomes the attraction, the system approaches the Mott MIT and Z recovers the standard behavior ($Z \rightarrow 0$). These trends are also more marked for $\lambda = 1.5$ where, as mentioned above, the system is a (bipolaronic) insulator in the absence of Hubbard repulsion, and a finite $U \gtrsim 1.2$ is required to have a metallic state. Most evident is of course the competition between U and the electron-phonon interaction, which becomes a sharp transition from $Z = 0$ for $U \lesssim 1.2$ to a maximum value $Z \simeq 0.5$ for $U \simeq 1.5$.

In the right panels of Fig. 8 we show the corresponding IEs α_Z , α_{Ω_0} . Also here the behavior of the isotope effect on the quasi-particle spectral weight is particularly interesting. In section III we have shown that giant IEs on the quasi-particle spectral weight Z are expected as the system approaches the bipolaronic metal-insulator transition. From an intuitive point of view we can expect that the electronic correlation, driving the systems far from the bipolaronic transition, reduces the magnitude of the anomalous IE α_Z . This picture is confirmed in Fig. 8 where we see that α_Z is strongly reduced as soon as U moves the system away from the bipolaronic MIT. This trend is however quite soon followed by a further enhancement of the anomalous IE on Z which becomes larger as the systems approaches the Mott transition, revealing that the strongly correlated regime close to the Mott metal-insulator transition is also highly sensitive to the phonon dynamics. This counterintuitive result can be qualitatively understood by following the analysis of Ref. 34 which showed that the strongly correlated regime close to the Mott MIT *in the presence* of electron-phonon interaction could be described in terms of a pure Hubbard model with a properly rescaled Hubbard repulsion $U_{\text{eff}} = U - \eta\lambda t$, where $\eta = 2\omega_0/(2\omega_0 + U)$. Since the quasi-particle spectral weight Z is known to scale linearly with $U_{c2} - U$ in DMFT for $U \rightarrow U_{c2}$, where U_{c2} is the critical value of the Hubbard repulsion at which a Mott metal-insulator transition occurs, we obtain thus

$$\alpha_Z = \frac{\lambda\omega_0 t U}{(U + 2\omega_0)^2 (U_{c2} - U_{\text{eff}})}. \quad (9)$$

This expression shows that the isotope effect on Z diverges as $1/Z$ as $U_{\text{eff}} \rightarrow U_{c2}$.^{34,36} The analytical behavior

predicted by Eq. 9, is also shown in the right-top panel of Fig. 8 (dashed lines). The critical values U_{c2} for each λ have been chosen in order to have the best fit with the DMFT numerical results: namely $U_{c2}/t = 2.87$ for $\lambda = 0.7$ and $U_{c2}/t = 2.90$ for $\lambda = 1.5$.

The crossover between the two different correlation regimes is also pointed out by the analysis of the behavior of the IEs on the renormalized phonon frequency α_{Ω_0} . Most evident is the case of $\lambda = 1.5$ where in the absence of Hubbard repulsion the ground state is a bipolaronic insulator. Here the non-monotonic behavior of α_{Ω_0} reflects two different regimes: *i*) a first sharp region $U \lesssim 1.36$ where $\alpha_{\Omega_0} \geq 0.5$. In this regime the system is characterized by a double-well lattice potential with a zero point energy larger than the barrier between the two minima as shown in Fig. 7b. By increasing ω_0 the system will probe thus a less shallow potential resulting in a stronger hardening of Ω_0 than the harmonic one and leading to $\alpha_{\Omega_0} > 0.5$. *ii*) for $U \gtrsim 1.36$, on the other hand, the shape of the lattice potential $V(x)$ is more similar to the panel (f) of Fig. 7 where the zero point energy is lower than the unstable minima. Increasing ω_0 the system would thus probe the flat potential regions around these two minima leading to an increase of the renormalized phonon frequency smaller than the harmonic one ($\alpha_{\Omega_0} < 0.5$). These effects become smaller as the Hubbard repulsion U increases since the minima shift higher in energy and the IE α_{Ω_0} approaches asymptotically 0.5 for $U \rightarrow \infty$.

A similar behavior occurs for $\lambda = 0.7$ where however the system in the absence of electronic correlation is still metallic although close to the bipolaronic MIT. In this case however increasing U leads to a reduction of the IE on Ω_0 until, for $U \gtrsim 0.85$, α_{Ω_0} becomes smaller than 0.5, although in a less marked way than in the $\lambda = 1.5$ case because of the smaller electron-phonon coupling. The evidence of this anomalous IE $\alpha_{\Omega_0} < 0.5$ even for small λ suggests thus that this regime is not related to the closeness to the bipolaronic metal-insulator transition. It is worth to stress in addition that the evidence of these two regimes of correlation prompts out from the analysis of the IE α_{Ω_0} while the renormalized phonon frequency itself Ω_0 does not show any signature of this crossover.

VI. CONCLUSIONS

In this paper we have studied in details the isotope dependence of several physical quantities: the quasi-particle spectral weight, the renormalized phonon frequency, and the static component of local charge and spin susceptibilities in the metallic regime of the Hubbard-Holstein model within DMFT approximation. The work is carried out for the half-filled model in the metallic phase without broken symmetries showing anomalous behaviors approaching the pair and the Mott metal-insulator transitions. We have shown that the anomalies of isotope coefficients can be helpful in revealing different physical regimes. In particular, we have found that

in the adiabatic regime $\gamma = 0.1$ we can identify two different regimes according to the degree of correlation. For $U \lesssim 1.5$ the physical properties of the system are qualitatively similar to those of the pure Holstein model where the approach to the bipolaronic metal-insulator transition obtained within DMFT is reflected in a near divergence of the IEs characteristic of bipolaronic binding. In this regime we find a divergent α_Z and a strong increase of α_χ close to the pair MIT while both α_{Ω_0} and α_ρ have a near divergence at λ_{ph} ($\alpha_{\Omega_0} \rightarrow +\infty$ and $\alpha_\rho \rightarrow -\infty$). The second regime establishes for $U \gtrsim 1.5$, where the bipolaronic MIT becomes of the first order.

The change in the order of the transition can be characterized in an accurate way by means of our study of IEs. In the highly correlated regime, the isotope effects are indeed not diverging even when the first-order transi-

tion is approached. The lack of any divergence as well as an analysis of the lattice potential suggest that the first-order character is more likely ascribed to an electronic mechanism than to a lattice-driven instability. In addition we have shown that approaching the Mott-Hubbard MIT also gives rise to drastic anomalous IEs.

Acknowledgments

We acknowledge useful discussions with C. Castellani, L. Pietronero and G. Sangiovanni. This work was partially funded by the MIUR project FIRB RBAU017S8R and PRIN projects 2003 and 2005.

-
- ¹ J. P. Franck, in *Physical Properties of High-Temperature Superconductors IV*, edited by D. M. Ginsberg (World Scientific, Singapore, 1994), p. 189.
- ² G. M. Zhao, M. B. Hunt, H. Keller, and K. A. Müller, *Nature (London)* **385**, 236 (1997).
- ³ R. Khasanov, D. G. Eshchenko, H. Luetkens, E. Morenzoni, T. Prokscha, A. Suter, N. Garifanov, M. Mali, J. Roos, K. Conder, and H. Keller, *Phys. Rev. Lett.* **92**, 057602 (2004).
- ⁴ M. Mali, J. Roos, H. Keller, A. V. Dooglav, Y. A. Sakhratov, and A. V. Savinkov, *J. Supercond.* **15**, 511 (2002).
- ⁵ M. Mali, J. Roos, H. Keller, J. Karpinski, and K. Conder, *Phys. Rev. B* **65**, 184518 (2002).
- ⁶ D. Rubio Temprano, J. Mesot, S. Janssen, K. Conder, A. Furrer, H. Mutka, and K. A. Müller, *Phys. Rev. Lett.* **84**, 1990 (2000); D. Rubio Temprano, J. Mesot, S. Janssen, K. Conder, A. Furrer, A. Sokolov, V. Trounov, S. Kazakov, J. Karpinski, and K. A. Müller, *Eur. Phys. J. B* **19**, 5 (2001).
- ⁷ G.-H. Gweon, T. Sasagawa, S. Y. Zhou, J. Graf, H. Takagi, D.-H. Lee, and A. Lanzara, *Nature (London)* **430**, 187 (2004).
- ⁸ C. Grimaldi, E. Cappelluti, and L. Pietronero, *Europhys. Lett.* **42**, 667 (1998).
- ⁹ E. Cappelluti, C. Grimaldi, and L. Pietronero, *Phys. Rev. B* **64**, 125104 (2001).
- ¹⁰ A. Deppeler and A. J. Millis, *Phys. Rev. B* **65**, 224301 (2002).
- ¹¹ T. Schneider, *Phys. Rev. B* **67**, 134514 (2003).
- ¹² P. E. Kornilovitch and A. S. Alexandrov, *Phys. Rev. B* **70**, 224511 (2004).
- ¹³ A. Bussmann-Holder, H. Keller, A. R. Bishop, A. Simon, R. Micnas, and K. A. Müller, *Europhys. Lett.* **72**, 423 (2005).
- ¹⁴ G. Seibold and M. Grilli, *Phys. Rev. B* **72**, 104519 (2005).
- ¹⁵ T. P. Devereaux, T. Cuk, Z.-X. Shen, and N. Nagaosa, *Phys. Rev. Lett.* **93**, 117004 (2004).
- ¹⁶ P. Paci, M. Capone, E. Cappelluti, S. Ciuchi, C. Grimaldi, and L. Pietronero, *Phys. Rev. Lett.* **94**, 036406 (2005).
- ¹⁷ O. Rösch, and O. Gunnarsson, *Phys. Rev. Lett.* **93**, 237001 (2004); *idem*, *Eur. Phys. Journal B* **43**, 11 (2005).
- ¹⁸ S. Fratini and S. Ciuchi, *Phys. Rev. B* **72**, 235107 (2005).
- ¹⁹ A. S. Mishchenko and N. Nagaosa, *Phys. Rev. B* **73**, 092502 (2006).
- ²⁰ For a review on this issues see for instance *High Temperature Superconductivity*, ed. by V.L. Ginzburg and D. Kirzhnits, Consultant Bureau, New York, London (1982), and references therein.
- ²¹ M.L. Kulić and R. Zeyher, *Phys. Rev. B* **49**, 4395 (1994).
- ²² M.L. Kulić, *Phys. Rep.* **338**, 1 (2000).
- ²³ E. Cappelluti, B. Cerruti, and L. Pietronero, *Phys. Rev. B* **69**, 161101 (2004).
- ²⁴ A. Georges, G. Kotliar, W. Krauth, and M. J. Rozenberg, *Rev. Mod. Phys.* **68**, 13 (1996).
- ²⁵ In the infinite coordination limit we rescale the hopping matrix element t as $t \rightarrow t/2\sqrt{z}$, so that the hopping amplitude t determines the half-bandwidth.
- ²⁶ M. Caffarel and W. Krauth, *Phys. Rev. Lett.* **72**, 1545 (1994).
- ²⁷ M. Capone and S. Ciuchi, *Phys. Rev. Lett.* **91**, 186405 (2003).
- ²⁸ M. Capone, P. Carta, and S. Ciuchi, *Phys. Rev. B* in press (2006) (cond-mat/0509542).
- ²⁹ Within DMFT the bosonic pairs that are formed in strong coupling have no dispersion. This leads to localization of such boson pairs, and to the metal-insulator transition. The bosons can instead move in finite dimensions, eventually leading to finite pair conductivity if the motion becomes coherent.
- ³⁰ A. J. Millis, R. Mueller, and B. I. Shraiman, *Phys. Rev. B* **54**, 5389 (1996).
- ³¹ W. Koller, D. Meyer, and A.C. Hewson, *Phys. Rev. B* **70**, 155103 (2004).
- ³² D. Meyer, A.C. Hewson, and R. Bulla, *Phys. Rev. Lett.* **89**, 196401 (2002).
- ³³ E. Cappelluti, C. Grimaldi, and L. Pietronero, *Eur. Phys. J. B* **30**, 511 (2002).
- ³⁴ G. Sangiovanni, M. Capone, C. Castellani, and M. Grilli, *Phys. Rev. Lett.* **94**, 026401 (2005).
- ³⁵ G.S. Jeon, T.-H. Park, J.H. Han, H.C. Lee, and H.-Y. Choi, *Phys. Rev. B* **70**, 125114 (2004).
- ³⁶ G. Sangiovanni, M. Capone, and C. Castellani, *Phys. Rev. B* **73**, 165123 (2006).